IOP Conf. Series: Journal of Physics: Conf. Series **1308** (2019) 012019 doi:10.1088/1742-6596/1308/1/012019

Observation of fission events in the ^{14}N+^{181}Ta system at projectile energies ≈ 5-6 MeV/A

Vijay R Sharma[1], R Kumar[2,⋆], B P Singh[3,†], E F Aguilera[1], Mohd Shuaib[3], S Mukherjee[4], R Dubey[5], P P Singh[6], S Kumar[2], S Appannababu[9], Abhishek Yadav[7], M K Sharma[8], J C Morales-Rivera[1], and R Prasad[2]

[1]Departamento de Aceleradores, Instituto Nacional de Investigaciones Nucleares, Apartado Postal 18-1027, Caixa Postal 11801, Distrito Federal, México
[2]NP-Group, Inter-University Accelerator Centre, New Delhi-110 067, India
[3]Department of Physics, Aligarh Muslim University, Aligarh 202 002, India
[4]Physics Department, Maharaja Sayajirao University of Baroda, Vadodara 390002, India
[5]iThemba LABS, National Research Foundation, P.O.Box 722, 7129 Somerset West, S. Africa
[6]Department of Physics, Indian Institute of Technology Ropar, Punjab-140 001, India
[7]Department of Physics, Jamia Millia Islamia, New Delhi-110025, India
[8]Department of Physics, Shri Varsheny College, Aligarh, Uttar Pradesh 202001, India
[9]Departamento de Fisica Nuclear, IF-Universidade de Sao Paulo, CEP 05508 090, Brazil

E-mail: ⋆rakuiuac@gmail.com, and †bpsinghamu@gmail.com

Abstract. Present paper reports the mass distribution of fission events in the ^{14}N+^{181}Ta reaction at four different projectile energies viz., 82.2 ± 0.8, 79.18 ± 0.82, 76.8 ± 1.2 and 72.9 ± 0.91 MeV using recoil catcher technique followed by off-line γ-ray spectrometry. A single peaked broad Gaussian mass curve has confirmed the nonappearance of any non-compound nuclear fission. Further, the variance of the mass distribution is compared with the existing literature data. It has been observed that the lower mass asymmetric system results in a lower variance of the mass distribution.

1. Introduction

The nuclear fusion process is defined as the capture of a projectile by the target nucleus forming fully equilibrated compound nucleus which subsequently decays by emission of particles followed by γ-rays to form evaporation residues (ERs). When the compound nucleus is heavy the fission process competes strongly with the evaporation of particles at each stage of the evaporation process, however, the role of the angular momentum (ℓ) transmitted to the target nucleus is also essential. For the values of ℓ above the critical angular momentum (ℓ_{crit}), the fission barrier decreases and an immediate fission process route may take place. This is also a limiting factor in the production of superheavy nuclei elements [1].

Recent experimental data on fusion [2, 3, 4, 5] at projectile energies 15% to 25% above the Coulomb barrier suggests the presence of fission events involving the projectiles such as ^{12}C,^{14}N,^{16}O and ^{20}Ne on medium mass targets, where fusion is expected to be a dominant mode of reaction process. In-spite of extensive work carried out for a wide range of excitation energy, and other entrance channel parameters [4, 6, 7, 8] a complete understanding of the

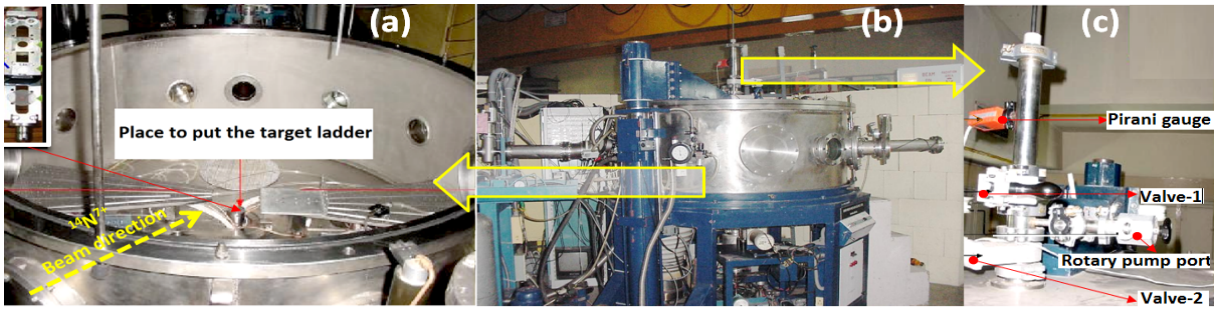

Figure 1. A typical snapshot of the General Purpose Scattering Chamber (GPSC) (a) inside view, target ladder is shown in the inset, (b) full view, and (c) In-vacuum transfer facility (ITF) setup view. For details see text.

mechanism of various types of reactions populated at low energies is still missing. Measurement of evaporation residues are signature of compound nucleus formation and useful probe to study the statistical as well as dynamical aspects of fusion-fission reactions.

For gaining a better insight into heavy ion reactions, a detailed study of the decay products of the compound nucleus ^{195}Hg in ^{14}N+^{181}Ta system has been undertaken by our group. A part of the data analysis involving fission events is reported in this paper.

2. Experimental Details

The experiment has been performed using $^{14}N^{6+,7+}$ beams from the 15UD pelletron accelerator at the IUAC, New Delhi, India. The thin Ta target foils ($\approx$ 99.9 %) of 1.3 to 1.9 mg/cm^2 and Al catchers of $\approx$ 1.4 to 2.0 mg/cm^2 were prepared using the rolling technique. Each target was followed by Al-catcher. Irradiations were performed in the GPSC of 1.5 m diameter having an in-vacuum transfer facility (ITF) using conventional recoil catcher technique. Using this ITF facility the samples after irradiation may be changed in the GPSC without disturbing the vacuum inside the chamber. Thus, the time lapse between the stop of the irradiation and the counting of the samples may be considerably reduced and thus induced activities of short half-lives may be recorded. Keeping in view the half-lives of interest ranging from few minutes to several hours, irradiations have been carried out for $\approx$ 8-10 hours. Typical photographs of the GPSC are given in figure 1 (a) inner view, target ladder in the inset, figure 1 (b) a full view of GPSC and figure 1 (c) the ITF setup. The flux of the incident ^{14}N ions was monitored using an ORTEC current integrator. The samples of ^{181}Ta alongwith appropriate catcher foil were irradiated at 82.2 $\pm$ 0.8, 79.18 $\pm$ 0.82, 76.8 $\pm$ 1.2, and 72.9 $\pm$ 0.91 MeV beam energies at a constant beam current $\approx$ 25 pnA. The activities produced in the samples were recorded off-line by HPGe detector of 100 c.c. active volume coupled to a CAMAC based software CANDLE [10]. The detector used in this experiment was pre-calibrated for energy and efficiency using various standard γ-sources viz., ^{60}Co, ^{133}Ba and ^{152}Eu at different source-detector separations. A typical plot of the photo peak efficiency of HPGe detector as a function of γ-ray energies varying from 121 keV to 1408 keV using ^{152}Eu point source at source-detector distance 3.0 cm, is shown in Fig. 2. It may be mentioned that the target-detector separation was suitably adjusted so as to keep the dead time $<$ 10 %. In order to detect and follow the residues of longer half-lives, the counting of irradiated samples has been done for several days. In the present work, we identified 22 fission events based on their characteristic energy of γ-lines and also from their measured half lives. For the sake of completeness a typical decay curve plot for an arsenic radio-isotope (^{70}As) is shown in figure 3. The measured half-lives of all the fission-like residues [13] were found to be in good agreement with their literature values [11].

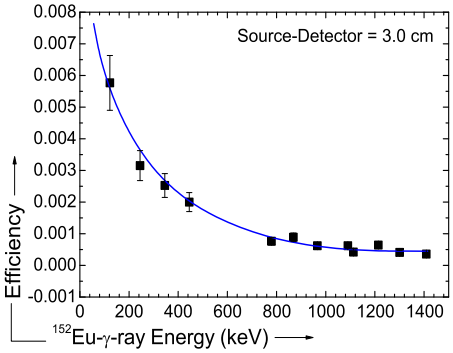

Figure 2. Typical plot of photo peak efficiency of HPGe detector as a function of γ-ray energy. The solid line is drawn to guide the eye.

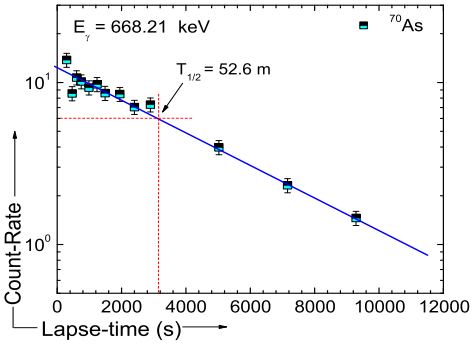

Figure 3. Typical decay curve of arsenic residue (^{70}As) at projectile energy 82.2 ± 0.8 MeV.

3. Data Reduction, Results and their interpretations

An experiment on the ^{14}N+^{181}Ta reaction suggesting the population of radio nuclide viz., ^{191}Hg, ^{190}Hg, ^{191}Au, ^{190}Au, ^{188}Pt, and ^{187}Pt via complete fusion (CF) and/or incomplete fusion (ICF) processes in the framework of theoretical model code PACE [12] has been reported recently [13]. Further analysis of the experimental data done in the present work revealed the presence of several residues which are not expected to be populated either by CF and/or ICF processes. These residues were found to have charge and atomic mass values around half of the values for the residues produced by composite systems formed as a result of fusion of projectile and the target nucleus, indicating the possibility of their production only through fission of composite systems. In a qualitative way, the fission arising due to the decay of the excited composite system formed via complete momentum transfer from projectile to the target nucleus may be termed as complete fusion-fission and via incomplete momentum transfer from the projectile to the target nucleus may be termed as incomplete fusion-fission. Though the identification of 22 fission-like events based on decay curve analysis as has been explained in the previous section, however, the formation cross-sections of such identified fission products is determined from the FORTRAN program EXP-SIGMA based on standard formulation described elsewhere [13] at 82.2 ± 0.8, 79.18 ± 0.82, 76.8 ± 1.2, and 72.9 ± 0.91 MeV beam energies. It may be pointed out that the overall error including statistical errors is estimated to be $\leq$ 15%, excluding the uncertainty in branching ratio, decay constant, etc., which have been taken from the Table of Radioactive Isotopes [11].

The plots of experimentally determined production cross-sections of various fission fragments at the studied energies are shown in figure 4 (a-d), respectively. The upward arrows indicate that only the metastable states have been measured and the total production cross-sections of these fission fragments are expected to increase. As can be seen in figure 4, the mass distributions of fission fragments are almost symmetric and can be fitted with one Gaussian function (as given in eq. 1) indicating the formation from the decay of compound nucleus.

$$Y(A) = \frac{Y_Z}{\sqrt{2\pi\sigma_A^2}} e^{-(A-A_p)^2/2\sigma_A^2} \quad (1)$$

where, the symbols have their usual meaning [14]. From eq.1, the parameter mass variance (σ^2) is obtained after the Gaussian fit and may be used to understand the behavior of stability of the decaying nucleus into fission via fissility. In order to explore this aspect, Itkis et al. [15] analyzed a large collection of data over a wide range of fissility of compound nucleus at medium

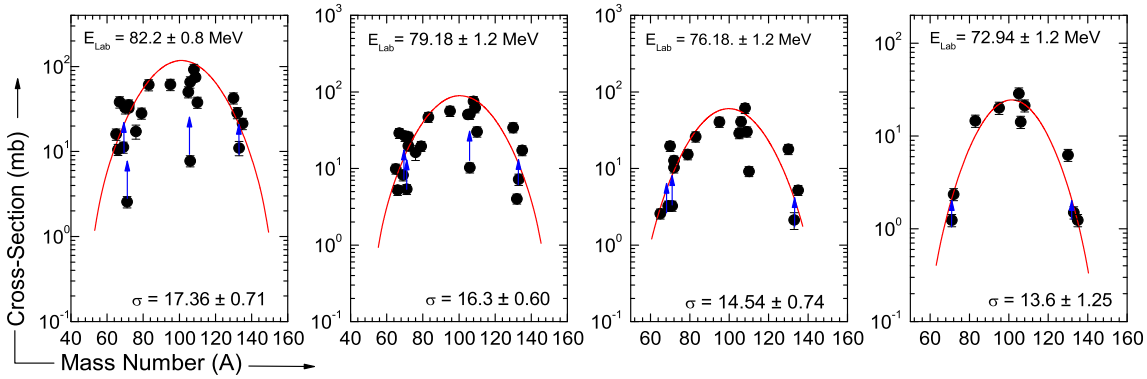

Figure 4. (Color Online) The plots of experimentally determined production cross-sections of various fission fragments at four different energies. The solid red line is the Gaussian fitting. The size of the filled circles includes the uncertainty in the yield values.

excitation energies. Moreover, the behavior of the stability (in terms of saddle point) for any system against the mass asymmetry (α) can be understood in the frame of Businaro-Gallone point (α_{BG}) [16], which is defined as the mass asymmetry for which the potential energy (saddle point) is maximum for a given fissility ($\chi = Z^2/A$). In the present work, the mass asymmetry (α=(A_T-A_P)/(A_T+A_P)) for the presently studied system is 0.856 and is found to be greater than the critical mass asymmetry ($\alpha_{BG} = 0.827$) of the system which suggests that the system will establish a mono-nuclear compact shape which facilitate equilibrium in all degrees of freedom and thus fission proceeds via compound nuclear processes and hence, the mass distribution is expected to be broad and symmetric.

Further, an attempt has been made to understand the role of entrance channel asymmetry on the behavior of mass distribution of fission-like fragments, the available mass variance of the fission fragments for different projectile-target combinations were compared with the presently calculated mass variance as a function of mass asymmetry (α). Figure 5 shows the distribution of the variance w.r.t α for four projectile-target combinations at constant projectile energy normalized with the Coulomb barrier (V_B). From the figure, it is noticed that the mass variance increases with the mass asymmetry of the interacting ions. This suggests a broader distribution of fission fragments for a more mass asymmetric system. However, more projectile-target combinations with different mass asymmetry values are needed to understand the dependence of mass variance on α.

In order to track the change in mass variance (σ^2) with excitation energy, the value of σ^2 obtained from the Gaussian fitting procedure of mass distributions of fission-like fragments is plotted as a function of excitation energy in figure 6. As can be seen in figure 6, the value of σ^2 increases with excitation energy, indicating larger spread in fission-fragment masses for higher excitation energies. The observed variation in the value of σ^2 with excitation energy for the present system follows the same trend as that reported by Ghosh et al. [19] in the above-barrier region for three different projectiles (^{19}F, ^{16}O, and ^{12}C) on a deformed target ^{232}Th (see figure 4(a-c) of Ref [19]). It may be mentioned that the present system was studied at only four energies above the barrier, hence the variation of the value of σ^2 with excitation energy at and below the barrier energies needs to be further investigated to better understand this aspect.

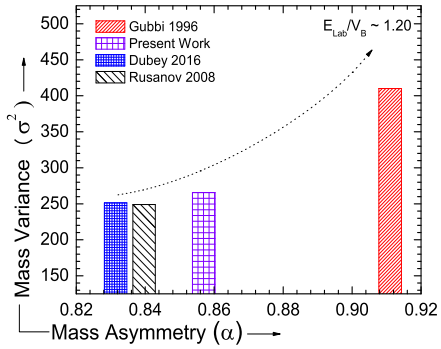

Figure 5. (Color Online) Mass asymmetry vs variances for the three projectile-target combinations (Gubbi 1996 [14], Dubey 2016 [17], Rusanov 2008 [18]). Dotted arrow is drawn to guide the eyes.

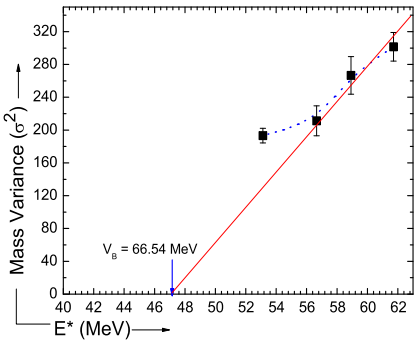

Figure 6. (Color Online) Mass variance as a function of excitation energy for ^{195}Hg. The red solid lines show the increase in σ^2 with excitation energy. Blue dotted line is drawn to guide the eyes.

4. Summary and Conclusions

The present paper reports the production cross-section of several fission fragments populated at four set of projectile energies. The mass distribution parameters obtained from the present measurements are studied in respect of mass asymmetry at constant normalized projectile energies. It has been observed that mass variance seems to exponentially increase with mass asymmetry but more experiments are required for different projectile and target combinations to explore the actual picture of the mass asymmetry systematics. The mass distribution of fission fragments at different excitation energies was studied to probe behavior of fission fragments.

5. Acknowledgments

The authors thank the Director of the IUAC, New Delhi, India for extending experimental facilities. VRS and EFA thank CONACYT for providing financial support under Project No. CB-01-254619. One of the author RD thanks SARCHI-DST, South Africa for financial support.

References

[1] Carlos A Bertulani Wiley Online Library, Nuclear reactions, 2014
[2] Tripathi R et al 2016 Phys Rev C **74** 014610
[3] Pal A et al 2018 Phys Rev C (R) **98** 031601
[4] Singh P P et al 2008 Int J Mod Phys E Vol 17, No3, 549-566
[5] Escher Jutta E et al 2012 Rev Mod Phys **84** 353-397
[6] Ngo Ch 1985 Prog Part Nucl Phys **16** 139
[7] Todd J R D et al 1993 J Phys G **19** 187
[8] Ramamurthy V S 1990 Phys Rev Lett **65** 25
[9] SRIM06: http://www.srim.org /
[10] CANDLE - Kumar B P Ajith et al 2001 DAE SNP, Kolkata
[11] Decay Radiation database version of 01 - 03 - 2018, http://www.nndc.bnl.gov/nudat2/
[12] Tarasov O B and Bazin D 2003 Nucl Instrum Methods Phys Res Sect B **204** 174
[13] Sharma V R 2019 Phys Rev C 99, 034617 (2019) and references therein
[14] Gubbi G K et al 1999 Phys Rev C **59** 3224-6
[15] Itkis M G et al 1995 Phys At Nucl **58** 2026
[16] Businaro U L and Gallone S 1995 Nuovo Cimento **1** 1277
[17] Dubey R et al 2016 Phys Lett B **752** 338-343
[18] Rusanov A Ya et al 2008 Phys At Nucl **71(6)** 956
[19] Ghosh T K et al 2005 Phys Lett B **627** 26